Ionics (2022) 28:2301–2307
https://doi.org/10.1007/s11581-021-04421-2

ORIGINAL PAPER

Constructing 2D Fe-doped CoP nanosheets for high-efficiency hydrogen evolution in alkaline media

Min Qian[1] · Xianfeng Tong[1] · Zixu Chen[1] · Wenhao Liao[1] · Yingyan Fu[1] · Haojiang Dai[1] · Qinghua Yang[2] · Tianyun Chen[1]

Received: 30 September 2021 / Revised: 13 December 2021 / Accepted: 18 December 2021 / Published online: 3 February 2022

Abstract

Designing and developing high-performance and low-cost non-precious metal electrocatalysts toward hydrogen evolution reaction (HER) are vitally desirable for future hydrogen application. Herein, we found that heteroatom doping was an effective method to improve the electrocatalytic performance of transition metal phosphide for HER. In this work, Fe-doped CoP nanosheets (NSs) were successfully prepared as an efficient HER electrocatalyst using a facile hydrothermal and phosphorization process. Specifically, the doping of Fe regulates the morphology of the catalyst, which can expose more active sites and modulate the electronic structures of CoP, thereby promoting the mass transfer kinetics of the HER process. With these advantages, the resultant $Fe_{1.5}$-CoP NSs (the doping amount of Fe is 1.5 wt %) exhibited outstanding HER catalytic activity to reach a current density of 10 mA cm^{-2} with a low overpotential of 115 mV, which dramatically outperforms that of pristine CoP. Moreover, the $Fe_{1.5}$-CoP NSs also displayed a good durability, which was proved by the 12-h chronoamperometry test.

Keywords Hydrogen evolution reaction · Electrocatalysts · 2D Nanosheets · Transition metal phosphides · Metal doping

Introduction

Hydrogen, an eco-friendly and renewable energy carrier, has been considered as one of the most potential alternatives to fossil fuels to solve environmental damage and energy crisis in the future [1–7]. Electrochemical water splitting is an environment-friendly and efficient strategy for hydrogen production. To date, precious metal Pt-based materials were viewed as the most efficient HER electrocatalysts [8–11]. However, high cost and scarcity of noble metals have greatly hampered their practical applications in a large scale [12, 13]. To this end, developing highly active, stable, and low cost non-noble metal electrocatalysts is extremely crucial and desirable [14–22].

So far, a range of non-noble metal electrocatalysts has been proved to be promising HER catalysts, such as transition metal borides, oxides, nitrides, carbides, and phosphides [23–27]. Among them, transition metal phosphides (TMPs) have been extensively studied in electrocatalytic field due to their structural similarity to hydrogenase [28–30]. Among the investigated TMPs, CoP has attracted wide attention because of its high conductivity, low-cost and high catalytic activities. However, the electrocatalytic performance of CoP still needs to be further improved when compared to noble metals due to the limited number of exposed active sites and poor charge-transfer ability [31–34]. Notably, studies have demonstrated that a proper introduction of different metal atoms into TMPs is an effective method to enhance the electrocatalytic activitity [35–37]. For example, Wang et al. reported that the Fe-doped Ni_2P nanosheet array exhibited a superior OER performance compared to the pure Ni_2P owing to the modulation of electronic structure [38].

Inspired by the work mentioned above, we designed and fabricated the Fe-doped CoP nanosheets (noted as Fe-CoP NSs) via a facile hydrothermal and subsequent phosphorization treatment. The resulting $Fe_{1.5}$-CoP NSs catalyst was characterized to possess large surface area, numerous active sites, favorable mass transfer kinetics, and short charge

✉ Tianyun Chen
t-y99@163.com

[1] School of Chemistry and Chemical Engineering, Hefei University of Technology, Hefei, Anhui 230009, People's Republic of China

[2] School of Food and Biological Engineering, Hefei University of Technology, Hefei, Anhui 230009, People's Republic of China

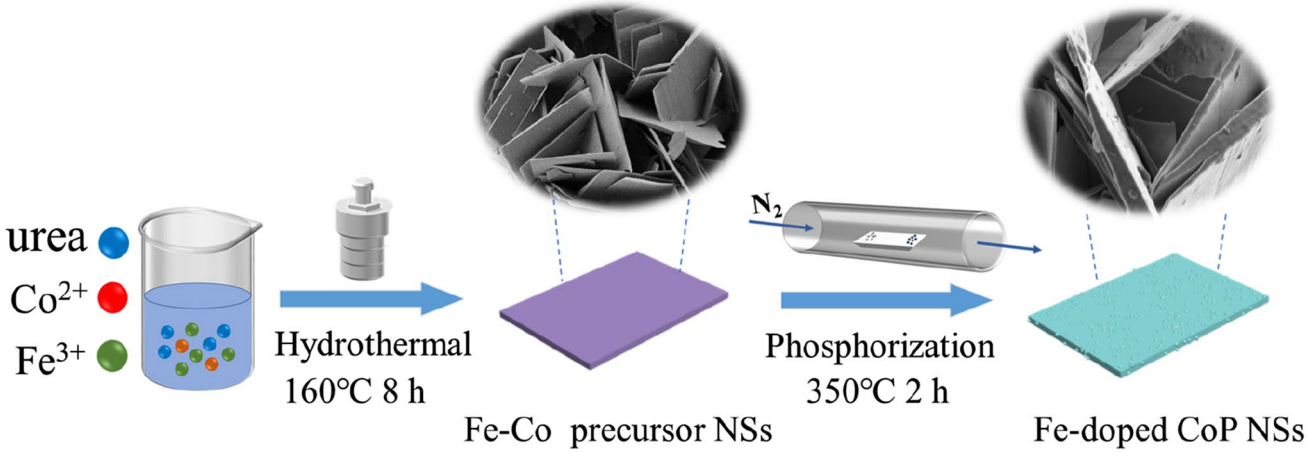

Scheme 1 Schematic illustration for the preparation process of Fe-doped CoP NSs

transport pathways, which facilitate the hydrogen evolution reaction. Satisfactorily, the Fe-doped CoP NSs showed superior catalytic performance towards HER in comparison with pure CoP. Meanwhile, benefiting from the nanosheets structure and the strong interactions between Fe and CoP, the Fe-doped CoP NSs with the doping amount of 1.5 wt % exhibited the best catalytic activity with a low overpotential of 115 mV to reach 10 mA cm^{-2}, outperforming the pristine CoP catalyst. Accordingly, this work provided an effective path for the widespread application of $Fe_{1.5}$-CoP NSs as HER electrocatalyst through a simple two-step fabrication.

Results and discussion

Scheme 1 illustrates the synthesis process of Fe_x-doped CoP nanosheets (Fe_x-CoP NSs). Firstly, Fe_x-Co precursors were fabricated by hydrothermal method, and Fe_x-CoP NSs samples were successfully prepared via low temperature phosphorization of the as-obtained precursors under N_2 atmosphere using NaH_2PO_2 as the phosphorus source.

The detailed microstructure and morphology features of $Fe_{1.5}$-Co precursors and $Fe_{1.5}$-CoP NSs samples were firstly observed by SEM and TEM images, as shown in Fig. 1. The SEM image in Fig. 1a indicated that the $Fe_{1.5}$-Co precursors were randomly arranged and regular nanosheet structure. As shown in Fig. 1b, the obtained $Fe_{1.5}$-CoP NSs inherited the nanosheet morphology of $Fe_{1.5}$-Co precursors with a thickness of about 130 nm, and nanoparticles appeared on the surface. The enlarged SEM image (Fig. 1c) more clearly displayed the nanoparticles on the surface of the nanosheet. In addition, the surface nanoparticles and the generated defects can also be further observed from the TEM image in Fig. 1d. In contrast, pure CoP without Fe doping remained a smooth nanosheet structure with a thickness of about 130 nm (Figs. S1 and S2).

The HRTEM image in Fig. 1e illustrated the interplanar distances of approximately 0.28 nm and 0.24 nm, corresponding to the (011) and (111) planes of CoP, respectively [39, 40]. The absence of FeP lattice also proved that the $Fe_{1.5}$-CoP NSs sample was composed of Fe-doping CoP instead of FeP/CoP composite [41]. The selected area electron diffraction (SAED) pattern in Fig. 1f ascribed to the (011), (111), (211), and (301) planes of the CoP, respectively, exhibiting the polycrystalline structure of CoP [42]. Additionally, the EDS spectrum of $Fe_{1.5}$-CoP NSs confirmed the co-existence of Fe, Co, P, and O elements (Fig. S3). And the elemental mapping in Fig. 1g–k further indicates the even distribution of Fe, Co, P, and O elements in $Fe_{1.5}$-CoP NSs, which also illustrated that Fe doping was homogeneous. Similarly, the HRTEM image and SAED pattern of pure CoP without Fe doping in Fig. S3 also confirmed the successful synthesis of CoP [43].

To further examine the crystal structure of the samples, the as-obtained Fe_x-Co precursors and Fe_x-CoP NSs were analyzed using X-ray diffraction (XRD) [42]. For the Fe_x-Co precursors (Fig. S4), the typical diffraction peaks matched well with that of bare Co precursors, and no other apparent impurity peaks were watched, manifesting that Fe was successfully doped into the Co precursors. After phosphorization, it can be seen that the diffraction peaks of pure CoP NSs at 31.6°, 36.31°, 48.13°, and 56.78° were indexed well to the (011), (111), (211), and (301) planes (JCPDS No:29–0497), respectively (Fig. 2a). In addition, the diffraction peaks of Fe_x-CoP NSs were consistent with that of CoP and no Fe-related phase was detected, which was in good agreement with the HRTEM results [44]. Figure 2b shows the nitrogen adsorption/desorption isotherm plot of $Fe_{1.5}$-CoP NSs, and the calculated BET specific surface area was 10 m^2 g^{-1}, which was larger than that of CoP NSs (Fig. S5, 4.72 m^2 g^{-1}). This larger BET surface indicated

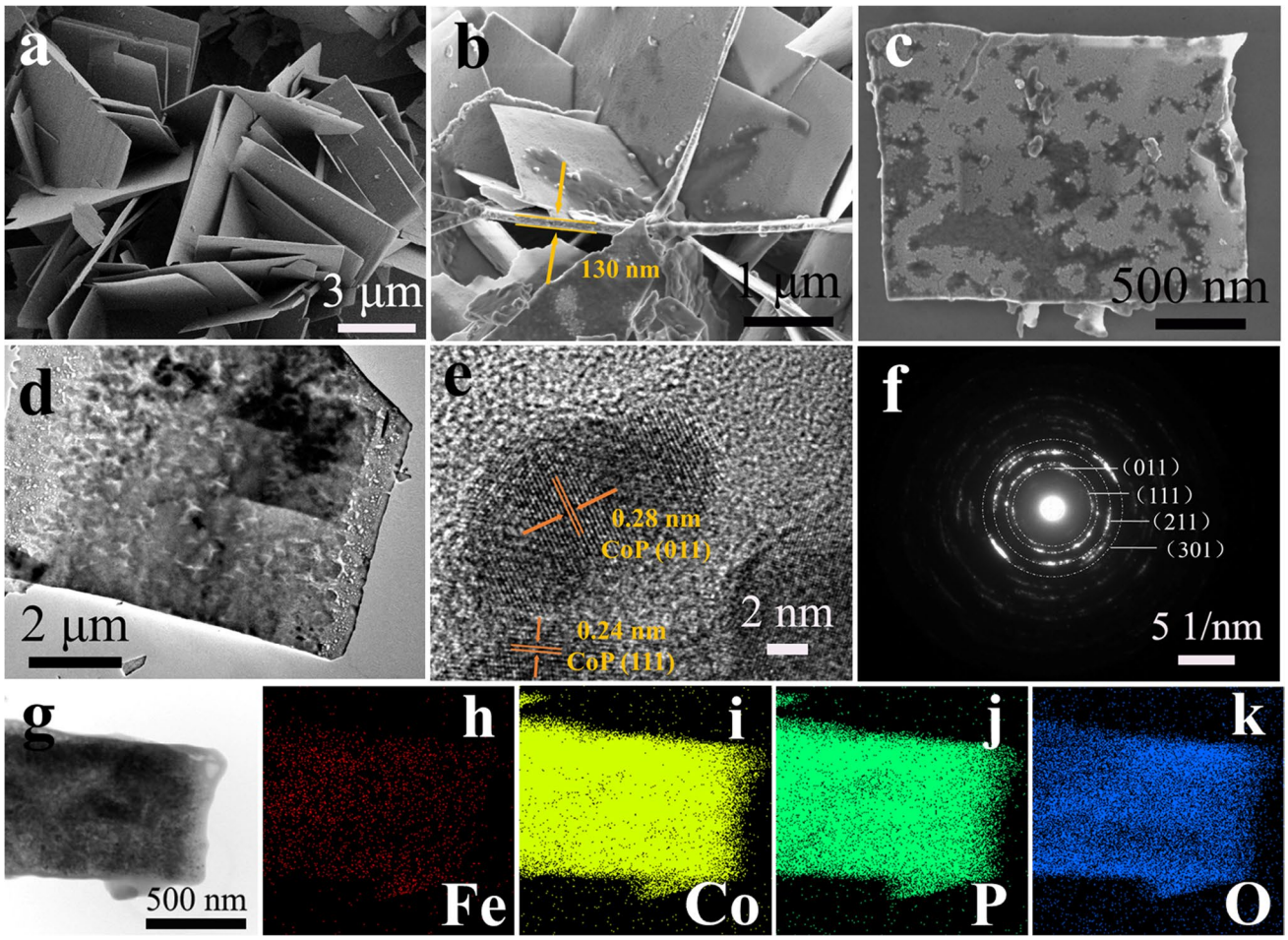

Fig. 1 SEM images of **a**, $Fe_{1.5}$-Co precursors; **b**, **c** $Fe_{1.5}$-CoP NSs; **c**, TEM image of $Fe_{1.5}$-CoP NSs; **e**, HRTEM image; **f**, SAED image and **g**–**k** corresponding element mapping of $Fe_{1.5}$-CoP NSs

that $Fe_{1.5}$-CoP NSs had a larger contact area and more active sites, which were favorable to enhance HER performance.

The valence states and elemental compositions of the $Fe_{1.5}$-CoP NSs electrocatalyst were further characterized by the X-ray photoelectron spectroscope (XPS). In Fig. 2c, the XPS survey spectrum clearly revealed the presence of Fe, Co, P, and O elements in $Fe_{1.5}$-CoP NSs, showing the consistency with the results of EDS. In the Co 2p spectrum of $Fe_{1.5}$-CoP NSs (Fig. 2d), the binding energies (BEs) at 778.6 and 782.1 eV can be assigned to Co $2p_{3/2}$, while the BEs at 793.3 and 798.2 eV were attributed to Co $2p_{1/2}$ [45]. And the clear peaks at 803.0 and 786.4 eV were attributed to the corresponding satellite peaks. Compared with CoP, it should be noted that the peaks of Co 2p in $Fe_{1.5}$-CoP NSs have a positive shift of 0.2 eV, which definitely revealed the strong interactions between Fe and CoP [46]. This modulated electronic structure in $Fe_{1.5}$-CoP NSs enabled the enhancement of HER performance.

For the Fe 2p region (Fig. 2e), the two peaks at 713.5 and 716.8 eV were assigned to the Fe $2p_{3/2}$ and Fe $2p_{1/2}$ for Fe^{3+}, and the peaks at 721.2 eV can be attributed to the satellite peaks of Fe 2p [47]. In the case of the O1s spectrum (Fig. S6), the O 1 s located at 530.8 eV indicated the formation of an M–O bond in the catalyst. And in general, the peak at 531.8 eV was caused by the hydroxyl oxygen, while the fitted peak at 533.1 eV can be corresponded to the P-O bond. As regards the P 2p spectra, which can be fitted with three peaks, as shown in Fig. 2f, the peaks at 129.5 and 130.2 eV were attributed to P $2p_{3/2}$ and P $2p_{1/2}$, respectively [48]. Meanwhile, the peak centered at 134.3 eV revealed the oxidized metal phosphate species because of the exposure to air. Comparing with the P 2p spectra of pure CoP NSs, it can be seen that the peaks of P 2p in the $Fe_{1.5}$-CoP NSs exhibited a weak negative direction shift, demonstrating that Fe doping can produce strong interactions between Fe, Co, and P [49]. In short, all the above XPS results revealed that Fe was doped into CoP successfully, and Fe doping can affect the electronic structure of CoP [44].

The electrocatalytic activity of CoP NSs and different Fe-doped CoP NSs toward HER was tested using a

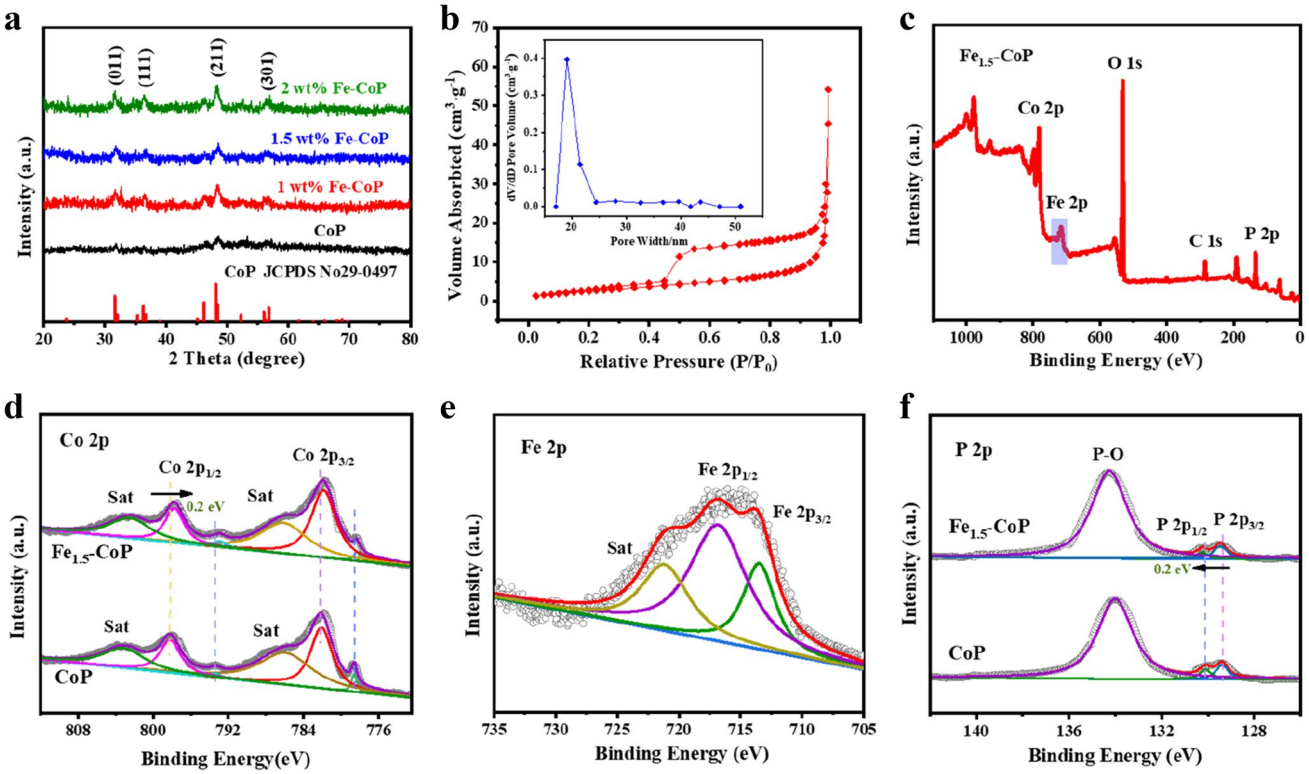

Fig. 2 **a** XRD patterns of Fe_x-CoP NSs. **b** N_2 adsorption–desorption isotherms of $Fe_{1.5}$-CoP NSs, and the inset is the corresponding pore size distributions. **c** XPS survey spectrum of $Fe_{1.5}$-CoP NSs. **d–f** High-resolution XPS spectra for Fe 2p, Co 2p, and P 2p of $Fe_{1.5}$-CoP NSs and CoP NSs

three-electrode system in 1.0 M KOH. Figure 3a shows the linear sweep voltammetry (LSV) curves of the set of samples. Pt/C catalyst exhibited the best catalytic activity having the smallest overpotential and Tafel slope. As expected, Fe_x-CoP NSs exhibited improved catalytic activity with a lower onset potential compared to CoP [48, 50]. Moreover, $Fe_{1.5}$-CoP NSs showed obviously superior HER performance among Fe_x-CoP NSs, requiring the smallest overpotential of 115 mV to deliver the current density of 10 mA cm^{-2}, in comparison to those of Fe_1-CoP NSs (142 mV), Fe_2-CoP NSs (187 mV), and CoP NSs (232 mV). This indicated that the introduction of Fe could remarkably enhance the HER performance. The Tafel slopes of various catalysts were calculated based on LSV to further explore the HER kinetics of $Fe_{1.5}$-CoP NSs. As shown in Fig. 3b, $Fe_{1.5}$-CoP NSs exhibited the lowest Tafel slope of 72 mV dec^{-1}, which was much smaller than those of Fe_1-CoP NSs (78 mV dec^{-1}), Fe_2-CoP NSs (82 mV dec^{-1}), and CoP NSs (104 mV dec^{-1}); thus, suggesting an appropriate amount of Fe doping in CoP played a great significant role in optimizing the performance of HER [51].

To further elucidate the intrinsic activity of Fe-doped CoP, electrochemical impedance spectra (EIS) measurements were performed in 1 M KOH. Generally, the value of charge transfer resistance (R_{ct}) varies inversely to the electrocatalytic reaction rate [52]. As seen in Fig. 3c, the R_{ct} of $Fe_{1.5}$-CoP NSs (16.7 Ω) was significantly smaller than that of Fe_1-CoP NSs (19.7 Ω), Fe_2-CoP NSs (42 Ω), and CoP NSs (46.3 Ω), suggesting a faster electron transfer rate for HER. Additionally, another key factor of the improved HER catalytic activity is the electrochemical surface area (ECSA), which can be roughly examined by electrochemical double-layer capacitance (C_{dl}) [53]. Figure S9 shows the cyclic voltammogram (CV) curves of CoP NSs and Fe-doped CoP NSs from 10 to 100 mV·s^{-1}; the C_{dl} values were obtained by calculation. Among them, the C_{dl} of $Fe_{1.5}$-CoP NSs was calculated to be 11 mF cm^{-2} (Fig. 3d), which was notably larger than those of Fe_1-CoP NSs (8.9 mF cm^{-2}), Fe_2-CoP NSs (6 mF cm^{-2}) and CoP NSs (2.3 mF cm^{-2}). As depicted in Fig. S10, $Fe_{1.5}$-CoP NSs showed the highest ECSA (550 cm^2) among all the investigated samples, signifying that it could provide abundant active sites to enhance the HER electrocatalyst performance [38].

Apart from good catalytic performance, HER long-term durability is other important factor to evaluate electrocatalysts. The stability of $Fe_{1.5}$-CoP NSs was evaluated by continuous cyclic voltammetry [41]. As depicted in Fig. 3e, negligible change was observed in polarization curves of

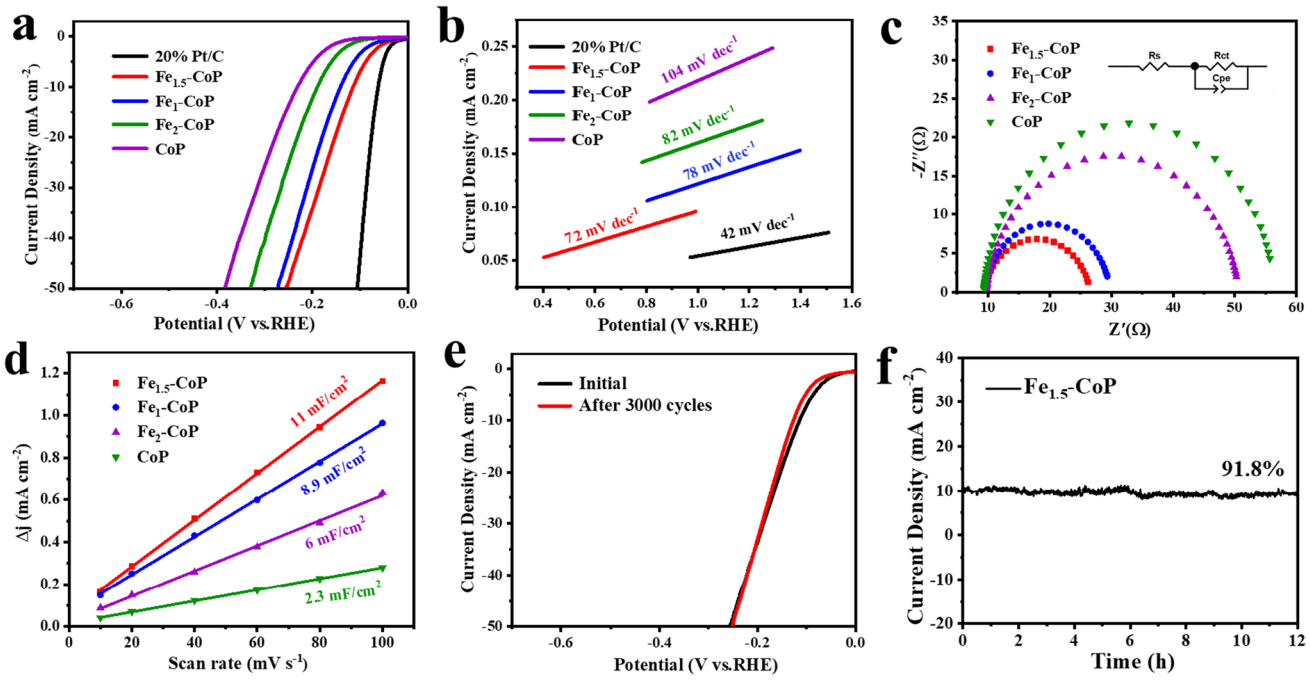

Fig. 3 **a** LSV curves of Pt, $Fe_{1.5}$-CoP, Fe_1-CoP, Fe_2-CoP and CoP NSs in 1 M KOH, **b** corresponding Tafel slopes, **c** EIS and **d** C_{dl} of different catalysts, **e** LSV curves of $Fe_{1.5}$-CoP NSs before and after 3000 cycles, **f** chronoamperometry curves of $Fe_{1.5}$-CoP NSs for HER

$Fe_{1.5}$-CoP NSs after 3000 cycles. Besides, the chronoamperometry measurement (Fig. 3f) revealed that $Fe_{1.5}$-CoP NSs exhibited a negligible degradation after continuous test for 12 h, and the LSV curve of $Fe_{1.5}$-CoP NSs (Fig. S11a) showed negligible shift, demonstrating its outstanding catalytic stability. Meanwhile, the XRD pattern in Fig. S11c exhibits no obvious crystal structure change and the morphology (Fig. S11b and S11d) of $Fe_{1.5}$-CoP NSs was entirely maintained after a long-term HER test. Furthermore, compared with the original spectrum in Fig. 2, the positions and intensities of the peaks relating to Fe 2p, Co 2p, P 2p, and O 1 s also showed no obvious changes (Fig. S12). These results further prove that $Fe_{1.5}$-CoP NSs had superior stability for hydrogen evolution reaction.

Conclusions

In summary, we reported a two-step method using hydrothermal and phosphorization treatment for the preparation of $Fe_{1.5}$-CoP NSs as an efficient HER electrocatalyst. Compared with pure CoP, the as-prepared $Fe_{1.5}$-CoP NSs showed significantly enhanced catalytic performance for HER, which can be ascribed to the electronic structure modulation led by proper introduction of Fe into CoP, which was confirmed by XPS results. Furthermore, the two-dimensional nanosheet structure also exposed a mass of active sites, which facilitated the HER process. Specifically, $Fe_{1.5}$-CoP NSs maintained a long-term extraordinary stability and durability after the continuous operation of 12 h. Therefore, this work provided a valid method for designing and fabricating low-cost and high-activity HER electrocatalysts, which is surely applicable for boosting the development of hydrogen industry.

Supplementary Information The online version contains supplementary material available at https://doi.org/10.1007/s11581-021-04421-2.

Funding This work was supported by Anhui Provincial Natural Science Foundation (1808085ME143) and the State Key Laboratory of Advanced Technology for Materials Synthesis and Processing (2021-KF-20, Wuhan University of Technology).

Declarations

Conflict of interest The authors declare no competing interests.

References

1. Chen T, Qian M, Tong X, Liao W, Fu Y, Dai H, Yang Q (2021) Nanosheet self-assembled NiCoP microflowers as efficient bifunctional catalysts (HER and OER) in alkaline medium. Int J Hydrogen Energy 46:29889–29895
2. Xing H, He W, Liu Y, Long G, Sun Y, Feng J, Feng W, Zhou Y, Zong Y, Li X, Zhu X, Zheng X (2021) Ultrathin and highly crumpled/porous CoP nanosheet arrays anchored on graphene boosts the capacitance and their synergistic effect toward

high-performance battery-type hybrid supercapacitors. ACS Appl Mater Interfaces 13:26373–26383
3. Dang Y, He J, Wu T, Yu L, Kerns P, Wen L, Ouyang J, Suib SL (2019) Constructing bifunctional 3D holey and ultrathin CoP nanosheets for efficient overall water splitting. ACS Appl Mater Interfaces 11:29879–29887
4. Ge Y, Chen J, Chu H, Dong P, Craig SR, Ajayan PM, Ye M, Shen J (2018) Urchin-like CoP with controlled manganese doping toward efficient hydrogen evolution reaction in both acid and alkaline solution. ACS Sustain Chem Eng 6:15162–15169
5. Qin S, Yao Y, Qian M, Yang Q, Chen T, Xu H, Zheng L (2020) Hierarchical microspheres composed of mn-doped CoP nanosheets for enhanced oxygen evolution. ACS Appl Nano Mater 3:10702–10707
6. Balaghi SE, Triana CA, Patzke GR (2020) Molybdenum-doped manganese oxide as a highly efficient and economical water oxidation catalyst. ACS Catal 10:2074–2087
7. Li X-X, Zhu P-Y, Li Q, Xu Y-X, Zhao Y, Pang H (2020) Nitrogen-, phosphorus-doped carbon–carbon nanotube CoP dodecahedra by controlling zinc content for high-performance electrocatalytic oxygen evolution. Rare Met 39:680–687
8. Stern L-A, Feng L, Song F, Hu X (2015) Ni_2P as a Janus catalyst for water splitting: the oxygen evolution activity of Ni2P nanoparticles. Energy Environ Sci 8:2347–2351
9. Wang J, Ciucci F (2019) In-situ synthesis of bimetallic phosphide with carbon tubes as an active electrocatalyst for oxygen evolution reaction. Appl Catal B 254:292–299
10. Liu X, Wei B, Su R, Zhao C, Dai D, Ma X, Xu L (2019) Mo-doped cobalt phosphide nanosheets for efficient hydrogen generation in an alkaline media. Energy Technol 7:1900021
11. Li L, Xu Q, Zhang Y, Li J, Fang J, Dai Y, Cheng X, You Y, Li X (2020) Low Ni-doped Co_3O_4 porous nanoplates for enhanced hydrogen and oxygen evolution reaction. J Alloys Compd 823:153750
12. Miao M, Zhang L, Zheng J, Ma W, Li H, Jiang S, Yu X, Huang Y, Gao J, Han G (2020) Urchin-like CoP nanomaterial as an electrocatalyst for efficient hydrogen evolution reaction. Int J Energy Research 45:4735–4745
13. Wu G, Chen W, Zheng X, He D, Luo Y, Wang X, Yang J, Wu Y, Yan W, Zhuang Z, Hong X, Li Y (2017) Hierarchical Fe-doped NiO_x nanotubes assembled from ultrathin nanosheets containing trivalent nickel for oxygen evolution reaction. Nano Energy 38:167–174
14. Tian H, Wang X, Li H, Pi M, Zhang D, Chen S (2019) Superhydrophilic Al-doped NiP_2 nanosheets as efficient electrocatalysts for hydrogen evolution reaction. Energy technol 8:1900936
15. Zhou P, Zhang Y, Ye B, Qin S, Zhang R, Chen T, Xu H, Zheng L, Yang Q (2019) MoP/Co_2P hybrid nanostructure anchored on carbon fiber paper as an effective electrocatalyst for hydrogen evolution. ChemCatChem 11:6086–6091
16. Ji P, Luo X, Chen D, Jin H, Pu Z, Zeng W, He J, Bai H, Liao Y, Mu S (2020) Significantly improved water oxidation of CoP catalysts by electrochemical activation. ACS Sustain Chem Eng 8:17851–17859
17. Shang L, Zhao Y, Kong X-Y, Shi R, Waterhouse GIN, Wen L, Zhang T (2020) Underwater superaerophobic Ni nanoparticle-decorated nickel–molybdenum nitride nanowire arrays for hydrogen evolution in neutral media. Nano Energy 78:105375
18. Xiao W, Zhang L, Bukhvalov D, Chen Z, Zou Z, Shang L, Yang X, Yan D, Han F, Zhang T (2020) Hierarchical ultrathin carbon encapsulating transition metal doped MoP electrocatalysts for efficient and pH-universal hydrogen evolution reaction. Nano Energy 70:104445
19. Jiang K, Luo M, Liu Z, Peng M, Chen D, Lu YR, Chan TS, de Groot FMF, Tan Y (2021) Rational strain engineering of single-atom ruthenium on nanoporous MoS_2 for highly efficient hydrogen evolution. Nat Commun 12:1687
20. Yao Y, Gu XK, He D, Li Z, Liu W, Xu Q, Yao T, Lin Y, Wang HJ, Zhao C, Wang X, Yin P, Li H, Hong X, Wei S, Li WX, Li Y, Wu Y (2019) Engineering the electronic structure of submonolayer Pt on intermetallic Pd_3Pb via charge transfer boosts the hydrogen evolution reaction. J Am Chem Soc 141:19964–19968
21. Yao Y, Hu S, Chen W, Huang Z-Q, Wei W, Yao T, Liu R, Zang K, Wang X, Wu G, Yuan W, Yuan T, Zhu B, Liu W, Li Z, He D, Xue Z, Wang Y, Zheng X, Dong J, Chang C-R, Chen Y, Hong X, Luo J, Wei S, Li W-X, Strasser P, Wu Y, Li Y (2019) Engineering the electronic structure of single atom Ru sites via compressive strain boosts acidic water oxidation electrocatalysis. Nat Catal 2:304–313
22. Yao Y, Wang S, Li Z, Wu Y (2021) Atomic level engineering of noble metal nanocrystals for energy conversion catalysis. J Energy Chem. https://doi.org/10.1016/j.jechem.2021.08.039
23. Men Y, Li P, Zhou J, Cheng G, Chen S, Luo W (2019) Tailoring the electronic structure of Co2P by N doping for boosting hydrogen evolution reaction at all pH values. ACS Catal 9:3744–3752
24. Wang B, Lu W-X, Huang Z-Q, Pan D-S, Zhou L-L, Guo Z-H, Song J-L (2020) A zeolite-type CoFe selenite via in-situ transformation of layered double hydroxide boosting the water oxidation performance in alkaline electrolyte. Chem Eng J 399:125799
25. Yue S, Wang S, Jiao Q, Feng X, Zhan K, Dai Y, Feng C, Li H, Feng T, Zhao Y (2019) Preparation of yolk-shell-structured Cox Fe1-x P with enhanced OER performance. Chemsuschem 12:4461–4470
26. Ma M, Zhu G, Xie F, Qu F, Liu Z, Du G, Asiri AM, Yao Y, Sun X (2017) Homologous catalysts based on fe-doped cop nanoarrays for high-performance full water splitting under benign conditions. Chemsuschem 10:3188–3192
27. Gao W, Yan M, Cheung H-Y, Xia Z, Zhou X, Qin Y, Wong C-Y, Ho JC, Chang C-R, Qu Y (2017) Modulating electronic structure of CoP electrocatalysts towards enhanced hydrogen evolution by Ce chemical doping in both acidic and basic media. Nano Energy 38:290–296
28. Chen T-Y, Zhang Y-Q, Fu Y-Y, Qian M, Dai H-J, Ye B, Qin S, Yang Q-H (2021) Construction of Ni–Mo–P heterostructures with efficient hydrogen evolution performance under acidic condition. J Mater Sci Mater Electron 32:14966–14975
29. Jiang D, Xu S, Quan B, Liu C, Lu Y, Zhu J, Tian DLi D, (2021) Synergistically coupling of Fe-doped CoP nanocubes with CoP nanosheet arrays towards enhanced and robust oxygen evolution electrocatalysis. J Colloid Interface Sci 591:67–75
30. Yang S, Lei G, Tan L, Xu H, Xiong J, Wang Z, Gu H (2021) Fe-doped MoO3 nanoribbons for high-performance hydrogen sensor at room temperature. J Alloys Compd 877:160200
31. Ma L, Liu Z, Chen T, Liu Y, Fang G (2020) Aluminum doped nickel-molybdenum oxide for both hydrogen and oxygen evolution reactions. Electrochim Acta 355:136777
32. Li W, Zhang S, Fan Q, Zhang F, Xu S (2017) Hierarchically scaffolded CoP/CoP_2 nanoparticles: controllable synthesis and their application as a well-matched bifunctional electrocatalyst for overall water splitting. Nanoscale 9:5677–5685
33. Guo M, Song S, Zhang S, Yan Y, Zhan K, Yang J, Zhao B (2020) Fe-Doped Ni–Co phosphide nanoplates with planar defects as an efficient bifunctional electrocatalyst for overall water splitting. ACS Sustain Chem Eng 8:7436–7444
34. Liao H, Sun Y, Dai C, Du Y, Xi S, Liu F, Yu L, Yang Z, Hou Y, Fisher AC, Li S, Xu ZJ (2018) An electron deficiency strategy for enhancing hydrogen evolution on CoP nano-electrocatalysts. Nano Energy 50:273–280
35. Liu J, Gao Y, Tang X, Zhan K, Zhao B, Xia BY, Yan Y (2020) Metal–organic framework-derived hierarchical ultrathin

CoP nanosheets for overall water splitting. J Mater Chem A 8:19254–19261
36. Sun Y, Hang L, Shen Q, Zhang T, Li H, Zhang X, Lyu X, Li Y (2017) Mo doped Ni2P nanowire arrays: an efficient electrocatalyst for the hydrogen evolution reaction with enhanced activity at all pH values. Nanoscale 9:16674–16679
37. Chen T, Qin S, Qian M, Dai H, Fu Y, Zhang Y, Ye B, Lin Q, Yang Q (2021) Defect-Rich Fe-Doped CoP nanosheets as efficient oxygen evolution electrocatalysts. Energy Fuels 35:10890–10897
38. Wang J, Ma X, Qu F, Asiri AM, Sun X (2017) Fe-Doped Ni_2P nanosheet array for high-efficiency electrochemical water oxidation. Inorg Chem 56:1041–1044
39. Guo C, Liu X, Gao L, Kuang X, Ren X, Ma X, Zhao M, Yang H, Sun X, Wei Q (2020) Fe-doped Ni_2P nanosheets with porous structure for electroreduction of nitrogen to ammonia under ambient conditions. Appl Catal B 263:118296
40. Tang C, Zhang R, Lu W, He L, Jiang X, Asiri AM, Sun X (2017) Fe-Doped CoP nanoarray: a monolithic multifunctional catalyst for highly efficient hydrogen generation. Adv Mater 29:1602441
41. Xu S, Qi Y, Lu Y, Sun S, Liu Y, Jiang D (2021) Fe-Doped CoP holey nanosheets as bifunctional electrocatalysts for efficient hydrogen and oxygen evolution reactions. Int J Hydrogen Energy 46:26391–26401
42. Zhang M, Ci S, Li H, Cai P, Xu H, Wen Z (2017) Highly defective porous CoP nanowire as electrocatalyst for full water splitting. Int J Hydrogen Energy 42:29080–29090
43. Zhou Q, Shen Z, Zhu C, Li J, Ding Z, Wang P, Pan F, Zhang Z, Ma H, Wang S, Zhang H (2018) Nitrogen-doped CoP electrocatalysts for coupled hydrogen evolution and sulfur generation with low energy consumption. Adv Mater 30:1800140
44. Li J, Zou S, Liu X, Lu Y, Dong D (2020) Electronically modulated CoP by Ce doping as a highly efficient electrocatalyst for water splitting. ACS Sustain Chem Eng 8:10009–10016
45. Yang F, Chen Y, Cheng G, Chen S, Luo W (2017) Ultrathin nitrogen-doped carbon coated with CoP for efficient hydrogen evolution. ACS Catal 7:3824–3831
46. Zhou L, Shao M, Li J, Jiang S, Wei M, Duan X (2017) Two-dimensional ultrathin arrays of CoP: electronic modulation toward high performance overall water splitting. Nano Energy 41:583–590
47. Xie J-Y, Liu Z-Z, Li J, Feng L, Yang M, Ma Y, Liu D-P, Wang L, Chai Y-M, Dong B (2020) Fe-doped CoP core–shell structure with open cages as efficient electrocatalyst for oxygen evolution. J Energy Chem 48:328–333
48. Qin X, Wang Z, Han J, Luo Y, Xie F, Cui G, Guo X, Sun X (2018) Fe-doped CoP nanosheet arrays: an efficient bifunctional catalyst for zinc-air batteries. Chem Commun (Camb) 54:7693–7696
49. Xu Y, Li X, Wang J, Yu Q, Qian X, Chen L, Dan Y (2020) Fe-Doped CoP flower-like microstructure on carbon membrane as integrated electrode with enhanced sodium ion storage. Chem Eur J 26:1298–1305
50. Wang X, Kolen'ko YV, Bao XQ, Kovnir K, Liu L (2015) One-step synthesis of self-supported nickel phosphide nanosheet array cathodes for efficient electrocatalytic hydrogen generation. Angew Chem Int Ed Engl 54:8188–8192
51. Xu P, Qiu L, Wei L, Liu Y, Yuan D, Wang Y, Tsiakaras P (2020) Efficient overall water splitting over Mn doped Ni_2P microflowers grown on nickel foam. Catal Today 355:815–821
52. Liu T, Ma X, Liu D, Hao S, Du G, Ma Y, Asiri AM, Sun X, Chen L (2016) Mn doping of CoP nanosheets array: an efficient electrocatalyst for hydrogen evolution reaction with enhanced activity at all pH values. ACS Catal 7:98–102
53. Hu E, Ning J, Zhao D, Xu C, Lin Y, Zhong Y, Zhang Z, Wang Y, Hu Y (2018) A room-temperature postsynthetic ligand exchange strategy to construct mesoporous Fe-doped CoP hollow triangle plate arrays for efficient electrocatalytic water splitting. Small 14:1704233